DOI: https://doi.org/10.37434/tpwj2024.08.02

MECHANICAL PROPERTIES OF THE REACTION-DIFFUSION BONDING OF THE HEAT-RESISTANT NICKEL-BASED ALLOY ChS70VI

V.E. Mazurak, M.O. Cherviakov, T.M. Kushnaryova, I.R. Volosatov

E.O. Paton Electric Welding Institute of the NASU
11 Kazymyr Malevych Str., 03150, Kyiv, Ukraine

ABSTRACT

The joint of the heat-resistant nickel-based alloy ChS70VI, obtained by the method of reaction-diffusion bonding during the formation of a weld by the melt of the heat-resistant nickel-based alloy with zirconium as a depressant is considered. The microstructures and concentration distribution of all chemical elements through the joint zone (with a gap width of ~20 μm and 50 μm) after the formation of the weld and subsequent heat treatment were analyzed. It is shown that the selected mode of heat treatment allows significantly reducing the amount of zirconium-rich eutectic phases (they are more easily melted, with a melting temperature of 960 °C), which increases the heat resistance of the joint. During heat treatment, the process of diffusion takes place, and the concentration of chemical elements in the weld is close to corresponding concentrations in the base alloy. Mechanical tests showed sufficiently high strength properties of the joint at temperatures up to 1100 °C. It was established that at the test temperature of 750°C, the strength of the joint is at the level of 95–98 % of ultimate strength of the base alloy.

KEYWORDS: heat-resistant nickel-based alloys, microstructure, mechanical properties, reaction-diffusion bonding, ChS70VI alloy, contact-reactive fusion, transient liquid phase bonding

INTRODUCTION

At present heat-resistant nickel-based alloys are an integral part in the field of construction of gas-turbine engines and power gas-turbine units. The good prospects and scope of application of these alloys directly depend on the possibilities of manufacturing concrete parts and structures of a complex shape that, in its turn, is due to the ability to join the respective alloys by permanent joints. A feature of heat-resistant nickel-based alloys is their extremely limited joinability by the traditional fusion welding methods. Such negative factors as higher sensitivity of the welded joints to hot cracking and local fracture in the overheating zone, lead to a considerable lowering of the welded joint properties [1]. Fusion welding, diffusion bonding and brazing are known as the main methods of repair and/or joining of the heat-resistant nickel-based alloys [2]. Each of these methods has certain limitations, so that the studies performed in this area both by local scientists and abroad remain to be relevant.

The method of reaction-diffusion bonding (RDB) in vacuum allows producing joints without autonomous melting of the base metal, eliminating the risk of macro- and microcrack formation, preserving the initial structure and avoiding the negative influence of the thermal cycle on physico-mechanical characteristics of the material being joined [3].

RDB method is based on formation of a liquid phase saturated with depressant (for Ni–Cr–Co system) and its penetration into a fixed gap between the planes being joined with its further crystallization and diffusion dissolution during heat treatment. The phenomenon of contact-reactive fusion of dissimilar metals is used to produce the liquid phase [4]. The liquid phase forms beyond the limits or directly near the gap between the parts being joined, as a result of contact-reactive fusion of the heat-resistant nickel-based alloy and depressant, and at certain bonding temperature it feels the gap under the action of the capillary forces. Zirconium in the form of foil was used as the depressant. In this capacity zirconium was studied and used in filler materials for brazing heat-resistant nickel alloys [5, 6].

THE OBJECTIVE OF THE WORK

is testing the method of reaction-diffusion bonding of heat-resistant nickel-based alloy ChS70-VI with a considerable area of weld edges, metallographic studies and assessment of mechanical characteristics of the produced joints.

INVESTIGATION MATERIALS AND METHODS

Investigations were conducted on joints of ChS70-VI alloy, which is the representative of the class of heat-resistant nickel-based cast alloys, and has been used for a long time already for manufacturing the hot section parts in power gas-turbine units. Blanks of 55×30×12 mm dimensions, cut out of one blank from ChS70-VI alloy were used to make the joints (Figure 1). Chemical composition of ChS70-VI alloy is given in Table 1. The gap of overall area of 660 mm^2

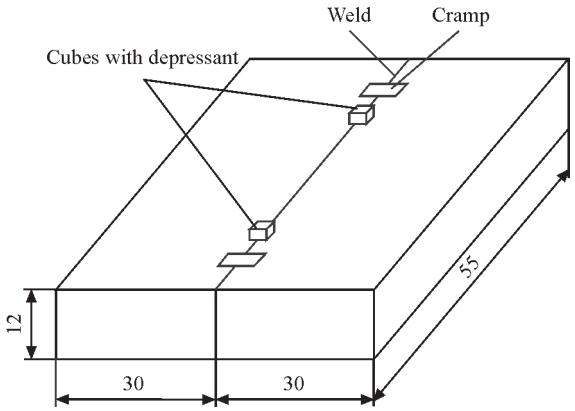

Figure 1. Scheme of assembly of a butt joint of ChS70-VI alloy

Table 1. Chemical composition of ChS70-VI alloy (TU 1-809-1040–96)

Weight fraction of elements, %								
C	Cr	Co	W	Mo	Al	Ti	Nb	Ni
0.06 0.12	15.0 16.7	10.0 11.5	4.5 6.0	1.5 2.5	2.4 3.2	4.2 5.0	0.1 0.3	Base

was filled with the liquid phase (based on Ni–Cr–Co system), saturated with zirconium. Before conducting RDB, the blanks were annealed at the temperature of 1050 °C for 2 h in vacuum. The abutted surfaces of the specimen were ground, and then butt joints were made. The uniformity of the fixed gap along the entire length of the specimen was provided by cramps from nichrome alloy, which were welded on the specimen surface by resistance spot welding. The cubes with zirconium foil were placed on top above the weld. They were also attached by resistance spot welding. The process of RDB of the assembled specimen (Figure 2, *a*) was conducted in a vacuum furnace in the following mode: heating up to the temperature of 1200 °C at the heating rate of 30–40 °C/min; soaking for 10 min, further cooling at the rate of 50–60 °C/min.

The appearance of the blank after RDB process showed complete wetting and filling of the gap along the entire length of the weld being made, with formation of grooves. Then, a piece of the joint was cut out

Figure 3. General view of MTS-810 testing machine

of the blank to conduct metallographic studies (Figure 2, *b*), and the rest of the specimen was subjected to diffusion annealing by the following mode: 1100 °C, soaking for 1 h; 1150 °C, soaking for 5 h. After that, part of the specimens were cut out for mechanical testing, and the rest of the joint metal was subjected to heat treatment by the following mode: 1050 °C, soaking for 3.5 h; aging at 860 °C, soaking for 17 h.

Microstructural investigations were conducted, using microhardness meter PMT-3 with 50 g load. Mechanical properties of the produced joints and base metal of ChS70-VI alloy were studied using MTS-810 servohydraulic machine (Figure 3). It consists of the following components: MTS 661.20F-02 dynamometer with axial load of up to 50 kN with the resolution of up to 0.1 N; MTS 632.53F-11 extensometer for operation with higher and high temperatures with 25 mm base and measurement resolution of 0.00001 %; MTS 653 Furnace with maximal temperature of specimen heating at testing of up to 1100 °C and three-zone monitoring with up to 5 °C tempera-

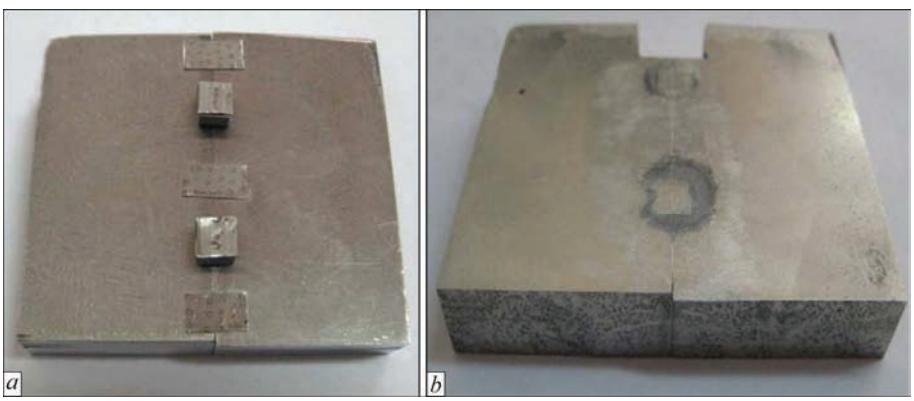

Figure 2. Specimen of a butt joint of ChS70-VI alloy before (*a*) and after joint formation at the temperature of 1200 °C for 10 min (*b*)

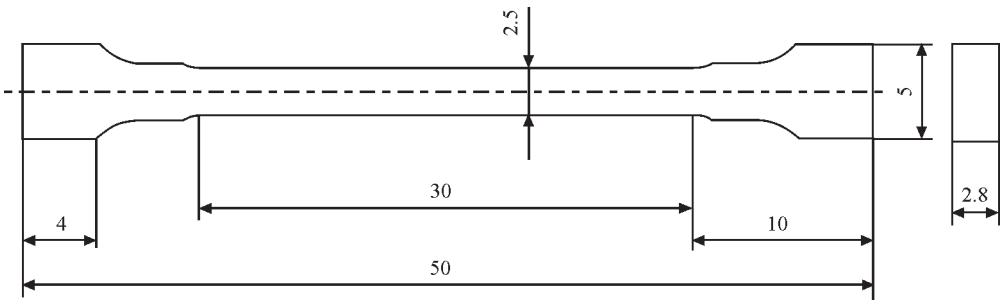

Figure 4. Specimen for short-time strength testing at room and high temperatures

ture gradient. Testing for short-term strength of the base metal and butt welded joints was conducted on flat specimens (Figure 4). Geometrical dimensions of the working length relative to the cross-sectional area and the initial length correspond to DSTU [7, 8] for room and higher temperatures, respectively. The strain rate during testing was equal to 0.00067 s^{-1}, which corresponds to the standards.

To conduct metallographic examinations the specimens were cut out normal to the weld. Polishing was performed using diamond paste and chromium oxide (III). Oxidation in air at the temperature of 350–400 °C was conducted to study the microsections in Neophot-32 optical microscope. The distribution of chemical elements was investigated by the method of local microX-ray spectral analysis, using energy-dispersive spectrometer Oxford Instruments X-max (80 mm^2), under the guidance of INCA software. The locality of the measurements was not greater than 1 μm. Shooting of the microstructures was conducted using scanning electron microscope TescanMira 3 LMU in backscattered electrons (BES), which allows examination of the microsections without chemical etching.

RESULTS AND DISCUSSION

METALLOGRAPHIC INVESTIGATIONS

Figure 5 shows the joint microstructures in the condition after the gap filling with the liquid phase and after diffusion annealing. Microhardness distribution across the weld before and after diffusion annealing (Figure 6) shows that the hardness of weld metal after conducting the full heat treatment became close to base metal hardness of 423 *HV* 0.05. However, in some regions of the weld of 50 μm width phases with hardness of both 480 *HV* 0.05 and 321 *HV* 0.05 remained after annealing. In the microstructures in Figure 5 one

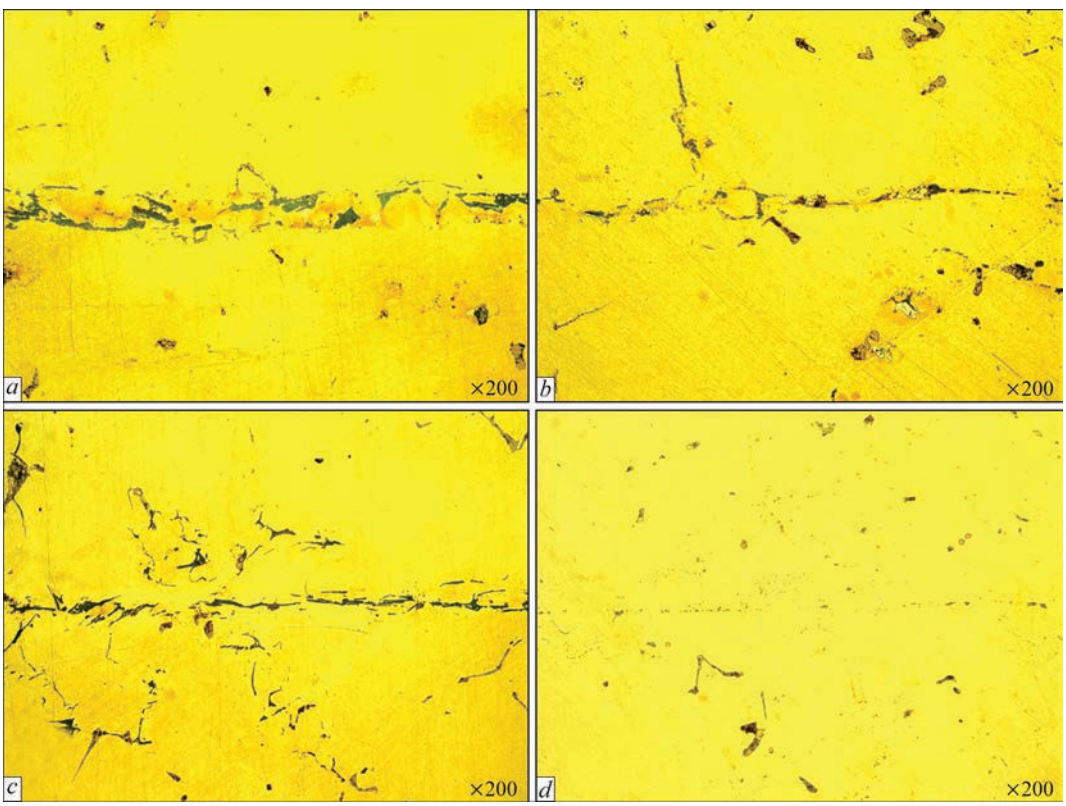

Figure 5. Microstructure (×200) of a butt joint of ChS70-VI alloy with gap width of ~50 μm (*a*, *b*) and ~10 μm (*c*, *d*), filled with liquid phase saturated with zirconium in the condition after heating up to 1200 °C, soaking for 10 min (*a*, *c*) and heat treatment at the temperature of 1100 °C, soaking for 1 h and 1150 °C, soaking for 5 h (*b, d*)

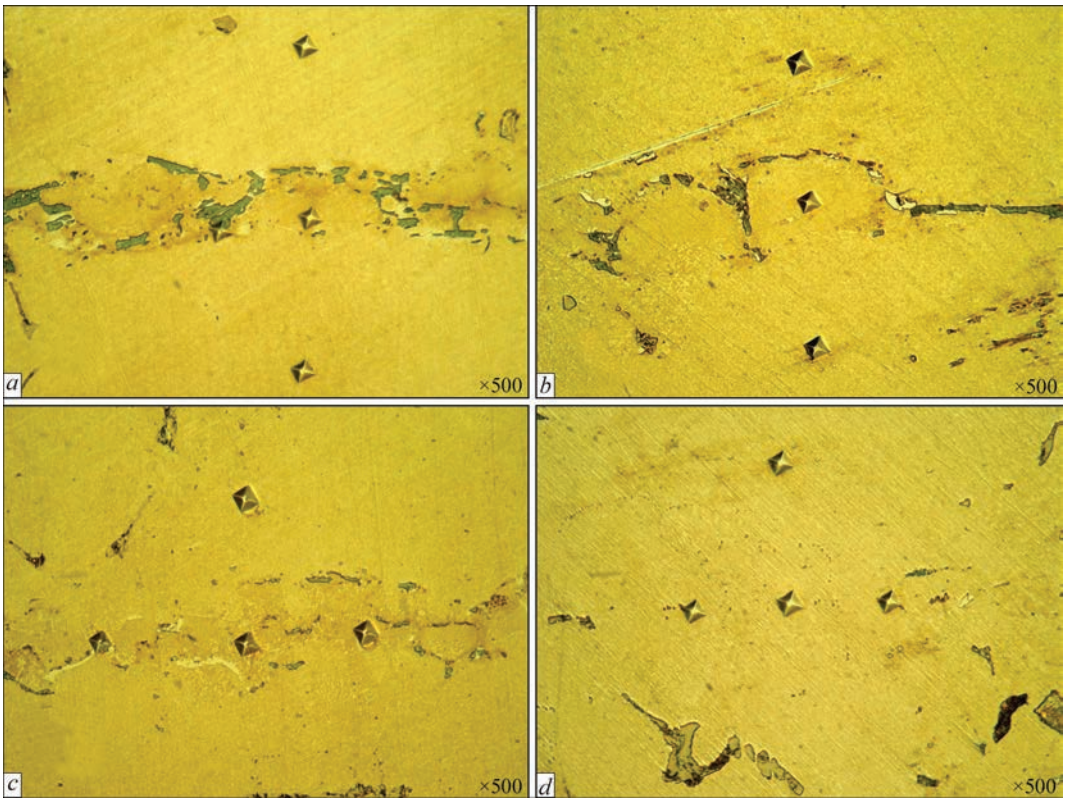

Figure 6. Measurement of *HV* microhardness (*P* = 50 g) across the weld 50 μm (*a, b*) and 20 μm wide (*c, d*) of the joint of ChS70-BI alloy, filled with the liquid phase saturated with zirconium in the condition after heating up to 1200 °C, soaking for 10 min (*a*, *c*) and heat treatment at the temperature of 1100 °C, soaking for 1 h and 1150 °C, soaking for 5 h (*b*, *d*) (×500)

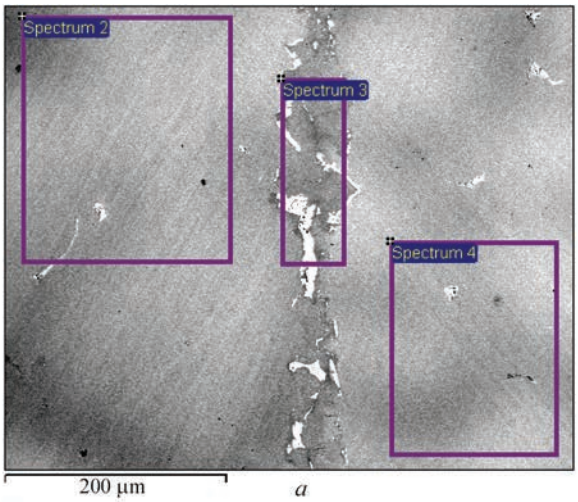

Spectrum	In the initial condition (1200 °C, 10 min)									
	Chemical element, wt.%									
	Al	Ti	Cr	Co	Ni	Zr	Nb	Mo	W	Total
2	2.64	3.13	13.23	8.74	66.52		0.19	1.44	4.11	100
3	2.65	4.21	12.46	7.05	63.50	1.79	0.71	2.52	5.11	100
4	2.91	3.81	13.27	8.43	66.49		0.44	1.73	2.93	100

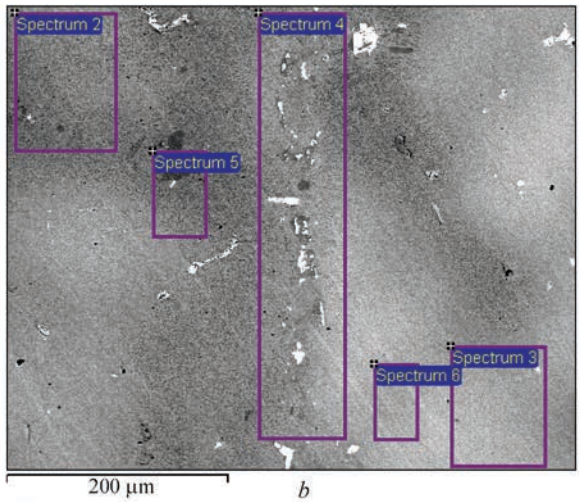

Spectrum	After diffusion annealing (1100 °C, 1 h + 1150 °C, 5 h)									
	Chemical element, wt.%									
	Al	Ti	Cr	Co	Ni	Zr	Nb	Mo	W	Total
2	2.60	4.28	13.78	9.24	64.80			1.89	3.41	100
3	2.40	3.56	14.7	9.79	64.34			1.83	3.38	100
4	2.83	3.78	14.09	9.03	64.22	1.24		1.57	3.24	100
5	2.89	5.3	12.44	8.65	67.49			1.46	1.77	100
6	2.54	3.27	14.86	9.77	62.20			1.56	5.80	100

Figure 7. Chemical composition of the weld zone (50 μm wide) and near-weld zone of the joint of ChS70-VI alloy, produced with application of zirconium depressant in the condition after formation of the joint at the temperature of 1200 °C, soaking for 10 min (*a*) and after homogenizing annealing at the temperature of 1100 °C, soaking for 1 h and 1150 °C, soaking for 5 h (*b*)

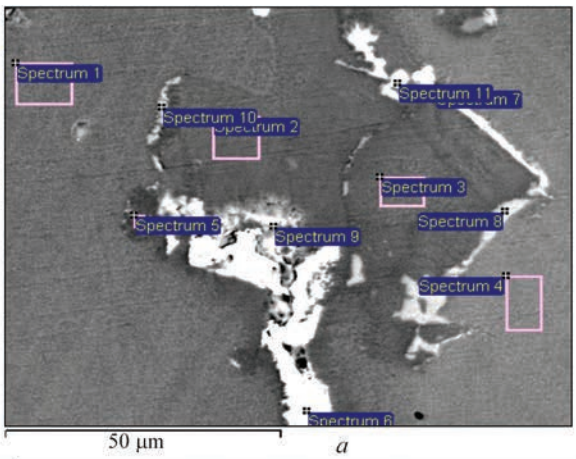

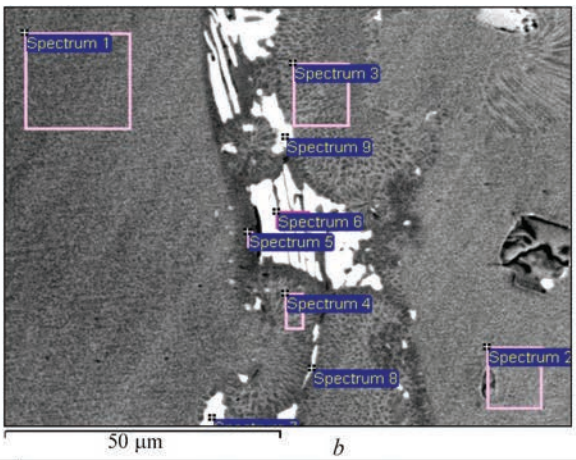

Spect.	Chemical element, wt.%									
	Al	Ti	Cr	Co	Ni	Zr	Nb	Mo	W	Total
1	2.80	3.35	12.82	8.48	67.12		0.01	1.45	3.96	100
2	3.10	3.71	12.73	8.21	67.79	0.55		1.45	2.46	100
3	2.88	3.79	12.96	8.08	67.87	0.55		1.35	2.52	100
4	2.75	3.05	13.34	8.63	65.67			2.07	4.49	100
5	3.48	5.62	7.58	6.87	73.05	1.13		0.66	1.61	100
6		2.08	35.89	1.51	3.26	1.39	1.91	23.53	30.44	100
7		1.29	37.96	1.78	17.83	1.12	0.80	14.96	24.25	100
8	0.52	1.30	1.97	5.17	63.48	26.63			0.93	100
9	3.27	12.67	6.44	5.57	60.11	2.40	3.22	1.60	4.72	100
10	0.79	2.11	6.87	5.48	60.40	22.04	1.11	1.20		100
11	0.21	1.07	49.87	1.68	5.79	0.82		15.77	24.79	100

Spect.	Chemical element, wt.%									
	Al	Ti	Cr	Co	Ni	Zr	Nb	Mo	W	Total
1	2.66	4.08	12.7	7.84	68.7			1.67	2.36	100
2	2.74	5.33	12.41	7.51	63.23	0.55	1.00	2.53	4.7	100
3	3.24	4.41	11.29	7.58	69.51			1.29	2.68	100
4	3.18	4.21	11.51	7.61	69.17	0.44		1.48	2.4	100
5	2.97	4.98	9.62	8.64	69.37	1.29	0.73	0.87	1.54	100
6	0.35	1.20	15.49	4.11	51.8	18.75	1.06	4.05	3.21	100
7	0.49	1.33	1.76	5.08	62.7	27.5	1.13			100
8	1.23	2.27	7.22	6.96	63.68	16.33	1.24	1.07		100
9	0.55	8.67	1.49	1.31	23.79	50.31	9.75		4.14	100

Figure 8. Chemical composition of individual phases of the weld and near-weld zone of the joint of ChS70-VI alloy, produced with application of zirconium in the condition after joint formation at the temperature of 1200 °C, soaking for 10 min

can clearly see that the applied heat treatment allows practically "resorbing" the weld 10–20 μm wide.

Figure 7 shows the structure and distribution of the concentration of all the elements through the zone of the joint ~ 50 μm wide in the condition after joint formation (1200 °C – 10 min) and after heat treatment (1100 °C – 1h + 1500 – 5 h). Studies were performed on a specimen with weld width of ~ 50 μm. One can clearly see that during heat treatment at 1100 °C for 1 h + 5 h at 1150 °C (which is just homogenizing) the weld width is noticeably reduced, the chemical composition and structure of the weld zone become close to that of the base material. It was established that the overall concentration of zirconium in the weld changed from 1.79 to 1.24 wt.%, i.e. zirconium diffusion into the base metal took place. Complete diffusion of zirconium from the weld into the base metal at the considered weld width requires not less than 20 h of homogenizing heat treatment. The final structure of the joint and, consequently, the strength of the formed joint depend on completeness of running of the processes of equalizing diffusion.

Comparative analysis of chemical composition of phases in individual regions of the joint zone before (Figure 8) and after (Figure 9) heat treatment on the studied length of 100 μm shows that the quantity of zirconium-rich phases (~22–26 wt.%, white phase) is markedly reduced. This phase represents the remains of the eutectic phase located between the common grains formed at RDB. Only small point islets of this phase remain after heat treatment. Here, the near-boundary zone of the weld has regions with zirconium content of 3–4 wt.% at 30–50 μm distance from the weld. (Ti + Zr) phase is observed in the weld and near-boundary zone both before and after heat treatment, with a high content of titanium (57.47 % Ti + 7.5 % Zr, 48.26 % Ti + 4.12 % Zr and 52.67 % Ti + 3.83 % Zr). Comparing the microstructures of the joint zone before and after vacuum annealing (Figures 8 and 9) one can come to the conclusion that a strengthening phase precipitated in the weld and its size is somewhat smaller than in the base metal. Judging from the nature of the results of X-ray spectral microanalysis (XSMA) phases enriched in W, Mo and Cr precipitate on the boundaries of crystallized grains. With the highest probability these are carbides of $Me_{23}C_6$ type [9, 10], precipitation of which is due to the alloy chemical composition during heat treatment.

Presence of Zr-rich phases in the weld (Figure 9) points to the completeness of running of Zr dissolution process in the alloy matrix, and the

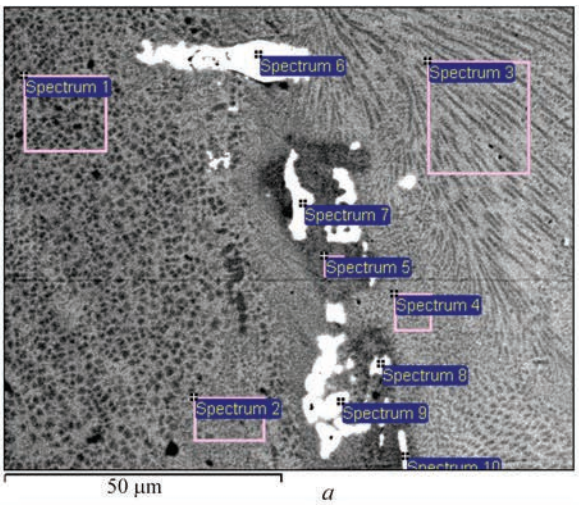

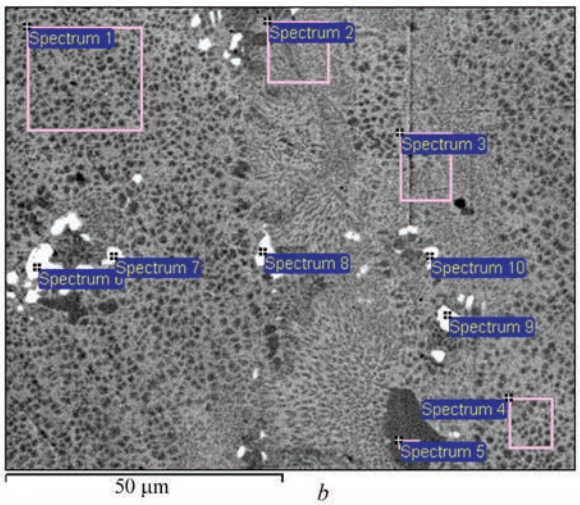

Spect.	Chemical element, wt.%								
	Al	Ti	Cr	Co	Ni	Zr	Mo	W	Total
1	2.8	4.39	14.01	8.77	66.34		1.57	2.1	100
2	2.91	3.65	14.69	8.74	64.29	0.69	1.68	3.36	100
3	2.37	3.48	14.57	9.32	63.45	0.51	2.02	4.28	100
4	2.85	3.34	14.35	9.03	64.39		2	4.04	100
5	3.14	5.26	10.78	8.8	67.15	1.47	1.19	1.64	100
6	1.01	57.49	0.89	0.66		7.5	2.79	5.82	100
7		1.5	2.03	5.88	60.62	29.03			100
8	1.17	2.08	3.12	6.64	61.53	24.4			100
9		6.78	1.99	1.5	5.72	73.78			100
10	0.65	1.92	4.63	6.25	61.55	24.02			100

Spect.	Chemical element, wt.%								
	Al	Ti	Cr	Co	Ni	Zr	Mo	W	Total
1	2.84	4.09	14.19	8.92	65.84		1.29	2.83	100
2	2.84	4.15	14.1	8.63	66.32		1.24	2.73	100
3	2.71	3.62	14.79	9.34	64.83		1.6	3.11	100
4	3.03	4.1	13.05	8.55	66.05	0.54	1.2	3.48	100
5	5.08	7.92	3.42	5.56	75.0	1.09		1.93	100
6	0.68	52.67	1.28			3.83	4.98	16.81	100
7		48.26	2.67	1.63	5.46	4.12	4.53	15.1	100
8	0.89	1.92	3.01	5.69	62.95	24.41			100
9		2.89	28.33	2.67	11.44	1.5	21.87	29.5	100
10	1.79	2.55	8.2	8.02	62.29	13.75	0.62	2.77	100

Figure 9. Chemical composition of the weld and near-weld zone of the joint of ChS70-VI alloy produced using zirconium, in the condition after homogenizing annealing in vacuum at the temperature of 1100 °C, soaking for 1 h and 1150 °C, soaking for 5 h

Table 2. Results of short-time strength testing of specimens of ChS70-VI alloy

Specimen	Specimen number	σ_t, MPa	$\sigma_{0.2}$, MPa	δ, %	T_{test}, °C	Fracture site
Base metal	1*	714.5	621.5	4.9	20	–
	2*	727.2	565.9	2.7	750	–
Joint	3*	701.9	657.3	2.1	20	Base metal
	4*	683.8	564.6	2.3	750	Weld
	5**	696.7	633.2	1.3	20	
	6**	781.3	656.8	6.3	20	Base metal
	7**	792.4	572.8	5.6	700	
	8**	729.6	575.2	2.7	800	Weld
	9**	526.1	383.3	12.7	900	
	10**	322.9	249.1	14.5	1000	
	11**	148.5	123.9	14	1100	Base metal
Base metal	32**	856.6	644.2	6.4	20	–
	33**	780.8	543.9	4.5	700	–
	34**	760.4	527.9	1.9	800	–
	35**	541.2	531.1	1.5	900	–
	36**	286.4	248.8	2.2	1000	–
	37**	140.7	121.9	8.3	1100	–

*Heat treatment: 1100 °C – 1 h + 1150 °C – 5 h.
**Heat treatment: 1100 °C – 1 h + 1150 °C – 5 h + 1050 °C – 3.5 h + 860 °C – 17 h.

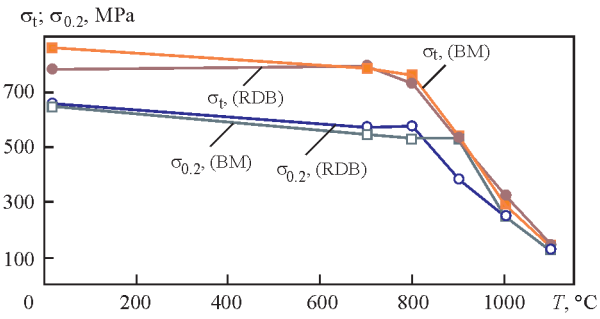

Figure 10. Temperature dependencies of ultimate strength σ_t and yield limit $\sigma_{0.2}$ of the base metal and butt specimens from ChS70-VI alloy produced by RDB method. Heat treatment is the same for all the specimens: 1100 °C – 1 h + 1150 °C – 5 h + 1050 °C – 3.5 h + 860 °C – 17 h

need to correct the joint gap width and the time of heat treatment duration.

MECHANICAL TESTING

Butt joints produced by RDB, before mechanical testing, were subjected to homogenizing annealing by the mode of 1100 °C for 1 h + 1150 °C for 5 h. Part of the specimens was additionally treated by two-stage aging at 1050 °C for 3.5 h + aging at 860 °C for 17 h. Testing was conducted in air at the following temperatures: 20, 750, 900, 1000, 1100 °C. The results are shown in Table 2. Specimens which additionally passed two-stage aging demonstrated a slight improvement of short-term strength and higher ductility at mechanical testing. For clarity, the data are also presented in the form of temperature dependencies of σ_t and $\sigma_{0.2}$ (Figure 10) and load diagrams (Figure 11).

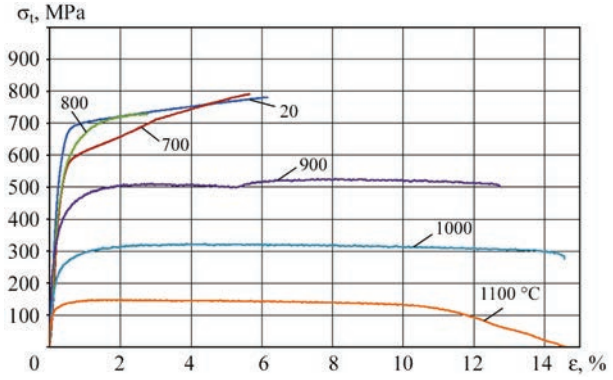

Figure 11. Load diagrams derived during short-time tensile testing of butt specimens from ChS70-VI alloy produced by RDB method with the following heat treatment: 1100 °C – 1 h + 1150 °C – 5 h + 1050 °C – 3.5 h + 860 °C – 17 h

Results of mechanical testing for short-term strength demonstrated a rather high level of weld strength, which is comparable with base metal level at the same heat treatment. Ultimate strength of RDB joints was equal to 91–100 % of that of the base metal, and the yield limit of RDB joints was equal to 95–100 % of that of the base metal. Figure 12 shows the broken specimens after testing. On part of the specimens with the joint the fracture ran through the base metal and not through the weld. This data indicate that homogenizing annealing at 1100 °C for 1 h + 1150 °C for 5 h led to dissolution of brittle intermetallics of zirconium, as well as diffusion of zirconium proper into the base metal, which is confirmed by metallographic examinations. The high strength and ductility (Figure 10, Figure 11) of RDB joints at test tempera-

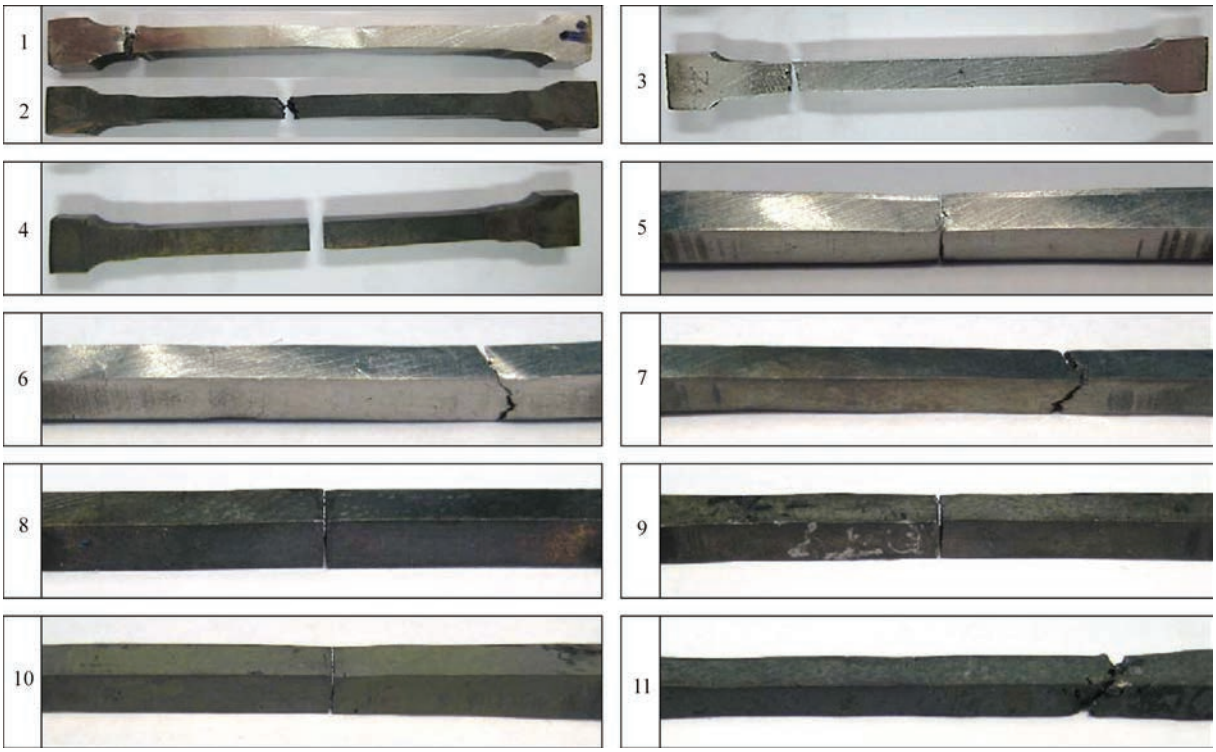

Figure 12. Appearance of specimens after destruction. Numbers on the left correspond to specimens shown in Table 2

tures of 1000 and 1100 °C (specimens 10 and 11), are also indicative (together with X-ray spectral chemical microanalysis) of the intensity of running of equalizing diffusion processes in the joint zone (weld and near-weld zone) and lowering of zirconium concentration in the weld during heat treatment. The lowest melting eutectic phases of intermetallics of Ni–Zr system have melting temperature of 960 °C ($NiZr_2$) and 1010 °C (NiZr) [11]. In the joints with weld width greater than 50 μm, the remains of such phases within the grain boundaries in the weld center can markedly lower their high-temperature strength.

CONCLUSIONS

A study was conducted with production of a butt joint of heat-resistant nickel-based ChS70-VI alloy by filling the gap with butt surface area of 660 mm^2 with the liquid phase formed during contact fusion of sintered powder of heat-resistant austenitic nickel-chromium alloy and metal of zirconium foil depressant. It is shown that at the temperature of 1200 °C the liquid phase has sufficient flowability and completely fills the joint gap.

Analysis of the structures and distribution of chemical elements in the base metal, weld and near-weld zone of the joint before and after homogenizing annealing revealed that the process of dissolution of some zirconium-rich intermetallic phases takes place, as well as carbide phase precipitation on the grain boundary. Concentrations of chemical elements in the weld are close to those in the base metal.

It is established that the strength properties of the joints at test temperatures of 750 °C correspond to 95–98 % of base alloy ultimate strength. Relatively high heat resistance of RDB joint has been achieved right up to the temperature of 1100 °C (maximal temperature of testing machine furnace).

REFERENCES

1. Kablov, E.N. (2001) *Cast blades of gas turbine engines (Alloys, technologies, coatings)*. Moscow, MISIS [in Russian].
2. Zhang, Y., Cheng, Y., He, N. et al. (2023) Microstructural characterization of TLP bonded joints of Mar-M247 superalloys with Ni–Cr–B interlayer. *Mater. Charact*., **198**, 112766 DOI: https://doi.org/10.1016/j.matchar.2023.112766
3. Nesmikh, V.S., Yushchenko, K.A., Kushnaryova, T.M. (2005) *Method of diffusion-reactive joining of metals and alloys.* Pat. Ukraine **73308** [in Ukrainian].
4. Lashko, S.V., Lashko, N.F. (1988) *Soldering of metals.* Moscow, Mashinostroenie [in Russian].
5. Kvasnytskyi, V.V., Myalnitsa, G.F., Matvienko, M.V. et al. (2019) Investigation of interaction of Ni_3Al-based alloy with interlayers of different alloying systems for TLP-bonding. *The Paton Welding J.,* **8**, 12–17. DOI: https://doi.org/10.15407/tpwj2019.08.03
6. Maksymova, S.V., Voronov, V.V., Kovalchuk, P.V. (2017) Brazing filler metal without boron and silicon for brazing of heat-resistant nickel alloy. *The Paton Welding J.*, **8**, 12–17. DOI: doi.org/10.15407/tpwj2017.08.02
7. (2020) DSTU ISO 6892-1:2019: *Metallic materials. Tensile testing.* Pt 1: Method of test at room temperature. Kyiv, SE UkrNDNTs [in Ukrainian].
8. (2021) DSTU ISO 6892-2:2020: *Metallic materials. Tensile testing.* Pt 2: Method of test at elevated temperature. Kyiv, SE UkrNDNTs [in Ukrainian].
9. Kishkin, S.T., Stroganov, G.B., Logunov, A.V. (1987) *Casting high-temperature nickel-based alloys.* Moscow, Mashinostroenie [in Russian].
10. Lashko, N.F., Zaslavskaya, L.V., Kozlova, M.N. et al. (1978) *Physico-chemical phase analysis of steels and alloys.* Moscow, Metallurgiya [in Russian].
11. (2001) *State diagrams of binary metal systems:* Refer. Book in 3 Vol. Ed. by N.P. Lyakishev. Moscow, Mashinostroenie [in Russian].

ORCID

V.E. Mazurak: 0000-0001-8671-348X,
M.O. Cherviakov: 0000-0003-4440-7665,
T.M. Kushnaryova: 0000-0003-1920-3118,
I.R. Volosatov: 0000-0003-2593-9869

CONFLICT OF INTEREST

The Authors declare no conflict of interest

CORRESPONDING AUTHOR

M.O. Cherviakov
E.O. Paton Electric Welding Institute of the NASU
11 Kazymyr Malevych Str., 03150, Kyiv, Ukraine.
E-mail: cherviakov@paton.kiev.ua

SUGGESTED CITATION

V.E. Mazurak, M.O. Cherviakov, T.M. Kushnaryova, I.R. Volosatov (2024) Mechanical properties of the reaction-diffusion bonding of the heat-resistant nickel-based alloy ChS70VI. *The Paton Welding J.*, **8**, 10–17. DOI: https://doi.org/10.37434/tpwj2024.08.02

JOURNAL HOME PAGE

https://patonpublishinghouse.com/eng/journals/tpwj

Received: 01.11.2023
Received in revised form: 27.05.2024
Accepted: 19.08.2024